MEASUREMENT OF DRIVING TERMS

F. Schmidt, R. Tomás, CERN, Geneva, Switzerland, A. Faus–Golfe, IFIC–Univ. of Valencia.

Abstract

In 2000 a series of MDs has been performed at the SPS to measure resonance driving terms. Theory predicts that these terms can be determined by harmonic analysis of BPM data recorded after applying single kicks at various amplitudes. Strong sextupoles were introduced to create a sizable amount of nonlinearities. Experiments at injection energy (26 GeV) with single bunch as well as one experiment at 120 GeV with 84 bunches were carried out. The expected nonlinear content is compared to the experimental observation.

1 INTRODUCTION

Since many years perturbation theory [1] and more recently the Normal Form [2,3] techniques have been used to understand nonlinear motion of single particles in hadron accelerators. This has proven to be very useful in the design phase of an accelerator. When it comes to existing machines these sophisticated tools have been rarely in use up to now. In part this is due to the complexity of the theory but also due to the fact that a nonlinear model of the accelerator cannot be easily predicted. Checking such a model experimentally [4] may prove even more difficult.

One well documented attempt to overcome this problem has been made by Bengtsson [5]. In the framework of the first order perturbation theory he has studied how the real spectra from tracking or experimental turn–by–turn data can be related to resonances. This study has stopped short of a complete solution. An important prerequisite to his analysis was a tune measurement technique superior to the standard FFT [6]. Similar attempts were performed in the field of celestial mechanics [7].

Recently, new techniques were developed [8], allowing an even more precise determination of the tunes. It seems therefore appropriate to review the link between experimental data and theoretical models. The frequency map analysis by Laskar [8] can be used not only to derive the tune, but also to find spectral lines in descending order of magnitude. It has already been shown how these spectra can be applied to remove from a sequence of tracking data unwanted regular complexity. Moreover, this method has been successfully used, again in tracking simulations, to correct resonances excited by sextupoles [9].

In this article we summarise our SPS experiments in 2000 which were done in the quest to establish this method as a tool for routine use in the control room.

2 SOME THEORY

The theory concerning single particle has been developed in Ref. [10]. A short outline for the case of single particles can be found in the next subsection. The second subsection describes how resonances are related to spectral lines. In the last subsection we give a shortened derivation of how a full particle distribution alters the results obtained for single particles.

2.1 Single Particle Formalism

Complex Fourier spectra of normalised coordinates can be written as:

$$\hat{x}(N) - i\hat{p}_x(N) = \sum_{j=1}^{\infty} a_j e^{i[2\pi(m_j\nu_x + n_j\nu_y)N + \psi_j]} \quad m_j, n_j \in \mathbf{Z}, \tag{1}$$

The connection between one–turn maps and Normal Form can be conveniently described using the Map–Normal Form Diagram (for details see [2,3]):

$$\begin{array}{ccc} \mathbf{x} & \xrightarrow{\mathbf{M}} & \mathbf{x}' \\ \mathbf{\Phi}^{-1}\big\downarrow & & \big\downarrow\mathbf{\Phi}^{-1} \\ \zeta & \xrightarrow[\mathbf{U}]{} & \zeta' \end{array} \tag{2}$$

Generating function F and Hamiltonian H are given by:

$$\mathbf{\Phi} = e^{:F(J,\phi):} \quad , \quad \mathbf{U} = e^{:H(J):} \quad . \tag{3}$$

The Normal Form coordinates can then be written as:

$$\zeta = e^{-:F_r:}\mathbf{h}, \quad h_z^{\pm} = \hat{z} \pm i\hat{p}_z, \tag{4}$$

with the generating function in resonance basis:

$$F_r = \sum_{jklm} f_{jklm}\zeta_x^{+j}\zeta_x^{-k}\zeta_y^{+l}\zeta_y^{-m} \tag{5}$$

or

$$F_r = \sum_{jklm} f_{jklm}(2I_x)^{\frac{j+k}{2}}(2I_y)^{\frac{l+m}{2}} \times e^{-i[(j-k)(\psi_x+\psi_{x_0})+(l-m)(\psi_y+\psi_{y_0})]}. \tag{6}$$

The generating function in action leads to:

$$\mathbf{h} = e^{:F_r:}\zeta = \zeta + [F_r,\zeta] + \frac{1}{2}[F_r,[F_r,\zeta]] + \cdots \tag{7}$$

The evolution of linearly normalised coordinates can be written as:

$$\begin{aligned} h_x^-(N) \quad = \quad & \sqrt{2I_x}e^{i(2\pi\nu_x N+\psi_{x_0})} \\ -2i\sum_{jklm} & j f_{jklm}(2I_x)^{\frac{j+k-1}{2}}(2I_y)^{\frac{l+m}{2}} \times \\ & e^{i[(1-j+k)(2\pi\nu_x N+\psi_{x_0})+(m-l)(2\pi\nu_y N+\psi_{y_0})]}. \end{aligned} \tag{8}$$

This expression relates the terms of the generating function and the spectral lines.

2.2 Resonance–Spectral Line Relation

A simple rule holds that says that for each resonance (n, m) there is a spectral line in the horizontal and vertical plane respectively:

- Horizontal Plane $(-[n-1], -m)$
- Vertical Plane $(-n, -[m-1])$

For example the (3, 0) resonance appears as a (–2, 0) line, the (1, 2) resonance is found as (0, 2) line, both in the horizontal spectrum. The skew resonance (0, 3) is not found in the horizontal spectrum, but appears as (0, –2) in the vertical spectrum.

2.3 Effect of Filamentation

In a real machine we will measure the centroid motion of particle distributions rather than single particle motion. For simplicity we restrict ourselves to treating horizontal motion only. A particle distribution right after such a horizontal kick by $\overline{A}_x$, where $\overline{A}_x = \beta_x * \Delta x'/\sigma$, takes the form:

$$\rho(I_x, \psi_{x0}) = \frac{1}{2\pi} e^{-(2I_x + \overline{A}_x^2 - 2\overline{A}_x\sqrt{2I_x}\cos(\psi_{x0}))/2} . \quad (9)$$

The Fourier transform $H_x^-(w)$ of the centroid which is the spacial integral of $h_x^-(N)$ from Eq. 8 can be written as:

$$H_x^-(w) = \int dN dI_x d\psi_{x0}\ \rho(I_x, \psi_{x0}) h_x^-(N) e^{-iwN} . \quad (10)$$

The tune is a function of amplitude and in first order of the horizontal invariant we get:

$$\nu_x = \nu_{x0} + \nu'_{xx} 2I_x . \quad (11)$$

The horizontal Fourier transform $H_x^-(w)$ is a sum over the components $H_{xjk}^-(w)$, with the horizontal line indices j and k:

$$H_{xjk}^-(w) = \begin{cases} \frac{-2ijf_{jk00}}{|m\nu'_{xx}|}(2I_x(w))^n e^{-\frac{1}{2}(2I_x(w)+\overline{A}_x^2)} \times \\ \quad \mathrm{I}_m(\overline{A}_x\sqrt{2I_x(w)}) \text{ , if } I_x(w) > 0 \text{ ;} \\ \\ 0 \text{ , if } I_x(w) \le 0 \text{ ,} \end{cases} \quad (12)$$

where we substituted the expressions containing j and k by:

$$\begin{aligned} n &= (j+k-1)/2 \\ m &= 1-j+k. \end{aligned} \quad (13)$$

I_m is the modified Bessel function of order m. Lastly, multiplying Eq. 11 by m and with $w = 2\pi m\nu_x$ (from Eq. 10) we define the function $I_x(w)$ as follows:

$$I_x(w) = \frac{1}{2m\nu'_{xx}}\left(\frac{w}{2\pi} - m\nu_{x0}\right) . \quad (14)$$

Considering evolving particle distributions instead of single particle motion turns the scalar quantity h_x^-, I_x into the distributions $H_{xjk}^-(w)$ and $I_x(w)$ respectively. Special attention has to be drawn to the fact that the factor $\frac{1}{m\nu'_{xx}}$ is present in both distributions. This means that the spectral lines taken from distributions are smaller than the expectation from single particle motion. In fact, lines corresponding to resonances of order $(j+k)$ are reduced by a factor $|m|$ (called decoherence factor in the following) of Eq. 13 after applying the normalisation with the tune line.

3 EXPERIMENTS AT SPS

3.1 Non–linear measurements at 120 GeV

Detuning

The detuning as a function of the square of the amplitude in the horizontal phase space ($\epsilon_x = A_x^2/\beta_x$) was measured and compared with the tracking model (Fig. 1). In absence of an exact knowledge of the octupole settings we used very weak excitations of them in the model to fit the detuning to the measured values. In the upcoming SPS experiments the influence of the octupoles will be further studied.

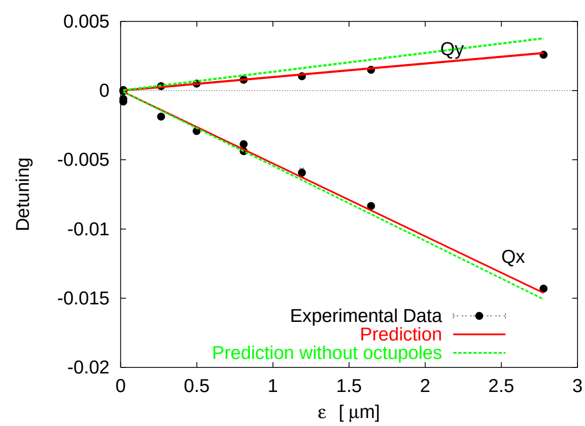

Figure 1: Detuning as a function of $\epsilon_x = A_x^2/\beta_x$.

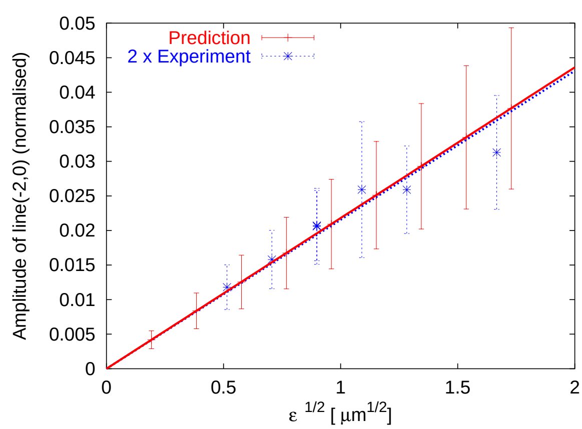

Figure 2: Resonance (3, 0) as a function of $\epsilon_x^{1/2}$.

Resonances (3, 0)

According to the last section the (3, 0) resonance corresponds to the (–2, 0) spectral line. In Fig. 2 the averages over the longitudinal positions of the experimental and the single particle model data are shown together with their σ value. As described in the last section the experimental data had to be multiplied by the the decoherence factor. In our case with $j = 3$ and $k = 0$ this decoherence factor has the value two. Both the average value and the sigma values of the experiment are in excellent agreement with the model data.

Localisation of Multipoles Contrary to the traditional belief the driving terms vary along the ring, in fact abrupt changes occur at the longitudinal locations of multipole kicks. In Fig. 3 this longitudinal variation of the (3, 0) resonance is compared between the model and the experimental data, for the latter the decoherence factor has been applied. In the upper graph the results are shown for that polarity of our intentionally strongly excited sextupole that seemed plausible compared to other SPS sextupole circuits. Much to our surprise we discovered that the two data sets were out of phase. The SPS operation experts later verified that the definition of the polarity of these special sextupoles was indeed opposite to that of the other circuits. Reversing the sign for these sextupoles in the model led to much better agreement as shown in the lower part of Fig. 3. To our knowledge this is the first example of how a driving term analysis can become useful to control nonlinearities in existing accelerators.

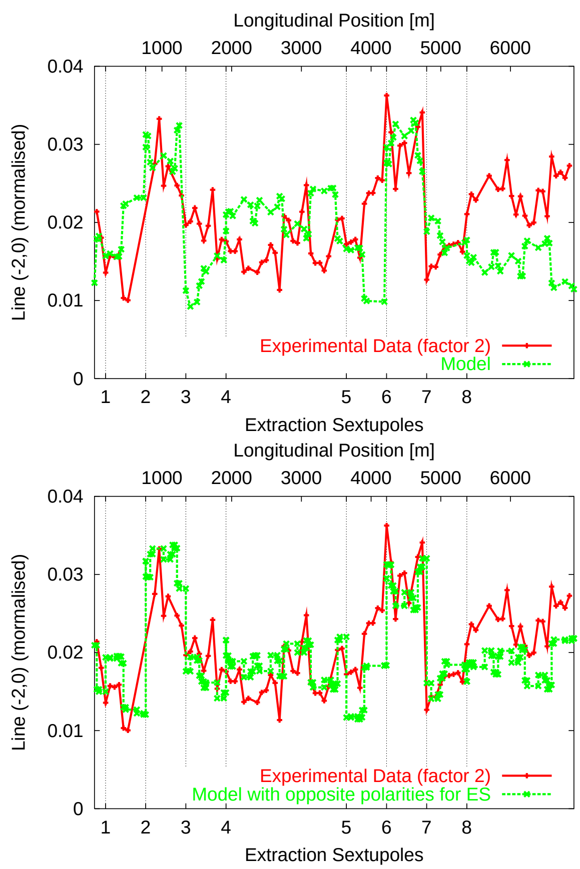

Figure 3: Longitudinal variation of the (3, 0) resonance.

3.2 Linear Coupling Compensation

Linear coupling is linked to the (1, -1) resonance which can be measured as the (0, 1) spectral line, i.e. the vertical tune line. Fig. 4 shows how the amplitude of the spectral line varies with the skew quadrupole strength. We could then demonstrate that the optimal skew quadrupole setting allowed a closest tune approach of $2 \cdot 10^{-4}$. It has to be noted that the change of slope from below to above the optimal skew quadrupole setting remains to be understood.

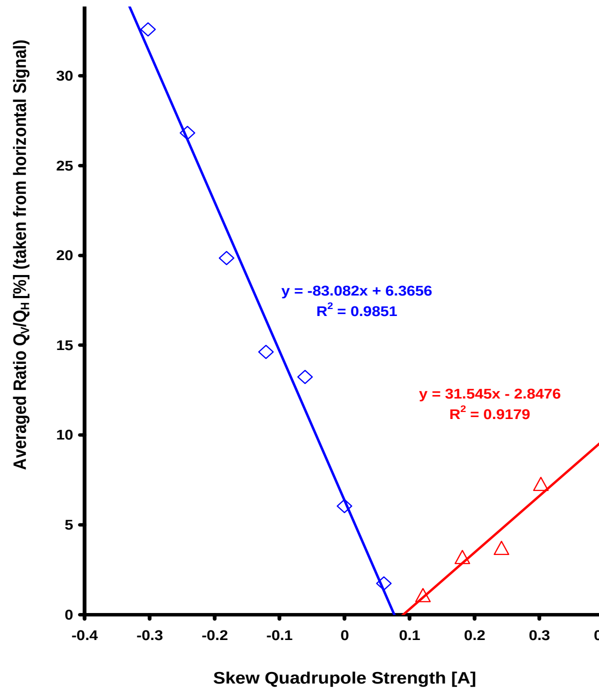

Figure 4: Linear Coupling compensation.

4 CONCLUSIONS

In last year's experiment at the SPS we could demonstrate for the first time that pick–up data allow the measurement of driving terms in an existing accelerator. In particular, the ability of measuring the longitudinal variation of resonances can be very useful to understand and steer an accelerator in the nonlinear regime. It is also of great value that the same tool allows to control linear features like the linear coupling to high precision. Although there are still some issues to be studied we believe that now the feasibility of this method for the use in the control room has been demonstrated.

5 REFERENCES

[1] A. Schoch, CERN 57–21, (1958).

[2] M. Berz et al., Part. Accel. **24**, pp. 91–107 (1989).

[3] A. Bazzani et al., CERN 94–02, (1994).

[4] O. Brüning et al., Part. Accel. 54, pp. 223–235 (1996).

[5] J. Bengtsson, CERN 88–05, (1988).

[6] E. Asseo et al., 4^{th} Euro. Signal Proc. Conf. (1988).

[7] J. Laskar, Astron. Astrophys. **198**, pp. 341–362 (1988).

[8] J. Laskar et al., Physica D **56**, pp. 253–269 (1992).

[9] R. Bartolini and F. Schmidt, AIP Conf. Proc. 395 (1996).

[10] R. Bartolini and F. Schmidt, Part. Accel. **59**(1998).